ONE-DIMENSIONAL MODELING OF MUD/DEBRIS UNSTEADY FLOWS

Ming Jin[1] and D. L. Fread [2]

ABSTRACT

The National Weather Service (NWS) one-dimensional dynamic flood routing model FLDWAV is enhanced to include capability of modeling mud/debris unsteady flows by including an additional friction slope term in the momentum equation of the Saint-Venant equations. Three techniques are incorporated into the model to determine the mud/debris related friction slope term due to the internal viscous dissipation of non-Newtonian fluids and granular sliding friction of coarse-grained debris surges. These techniques are tested and some computational results are compared with observed field data and experimental data.

INTRODUCTION

Mud/debris floods, such as those caused by landslide-induced mud/debris flows or those emanating from the dam-break-failure of tailings or debris dams, are unique unsteady flow phenomena in which the flow changes rapidly and the properties of the moving fluid mixture of mud/debris and water are very different from those of pure water floods. Since mud/debris flows are rarely steady or uniform, unsteady flow modeling is of practical significance. At present, models that employ hydraulic simplifications provide the most sophisticated tool for practical predictions of mud/debris flow runouts and inundation limits. Such models also have scientific importance because at present they constitute the state-of-the-art method for predicting unsteady nonuniform motion, the mud/debris flow's most obvious and readily measured attribute. One hydraulic method of modeling mud/debris flows is to use the one-dimensional dynamic unsteady flow equations in which an additional friction slope term is included in the conservation of momentum equation. The derivation of the friction slope term for the mud/debris flow depends on the particular resistance formulation used to represent the effect of the non-Newtonian fluid's internal viscous friction , the fluid mixture's solid-liquid interaction due to granular sliding, and nonhydrostatic pore-pressure distribution of non-homogenous solid-liquid mixture.

Compared with an open channel flow of pure water whose resistance behavior is

---

[1]Visiting Scientist, Hydrologic Research Laboratory, Office of Hydrology, National Weather Service, 1325 East-West Hwy.,Silver Spring, MD 20910
[2]Director, Office of Hydrology, National Weather Service.

mainly attributed to the boundary turbulent shear stresses and therefore the mechanisms of momentum transport and energy dissipation are essentially universal, the resistance behavior of the mud/debris flow depends on the relative importance of the shear stresses arising from such different sources as: (1) the turbulent shear stress due to the channel boundary roughness; (2) the solid-liquid mixture's viscous stress and yield stress; (3) the mixture's dispersive stress due to sustained frictional contacts; (4) the inelastic collisions of solid particles within the fluid mixture. Consequently, the characteristics of mud/debris flows may differ significantly between events. For the purpose of hydraulic modeling, the unsteady mud/debris flows can be roughly classified as either mud floods, viscous mudflows or granular debris flows (Julien and O'Brien, 1997). Different resistance modeling techniques may be used for different situations. Mud floods can be modeled using the same resistance technique as for water floods, i.e., one that accounts for turbulent shear stresses, only. In this paper, three techniques are developed to model the special resistance behavior of mud/debris flows, i.e. (1) a viscoplastic technique for modeling mudflows, (2) a granular sliding technique for modeling debris flows, and (3) a combined resistance coefficient technique (pseudo Manning's n) for modeling mud/debris flows. Each of these techniques are presented, tested, and compared. The model application limitations are studied and computational results are compared with observed field data and some large-scale experimental data.

The NWS FLDWAV model is a generalized dynamic flood routing model based on the numerical solution of the one-dimensional unsteady flow (Saint-Venant) equations using selected numerical schemes, i.e. (1) an implicit weighted four-point, nonlinear, finite-difference scheme and (2) an explicit characteristics-based upwind scheme. Also, level pool routing and/or diffusion routing can be selected for various portions of an entire routing reach. FLDWAV combines the capabilities of the popular NWS DAMBRK and DWOPER models (Fread,1993) while providing several additional modeling capabilities. This study incorporates the three mud/debris flow modeling techniques into the FLDWAV model. These techniques are user selected options to deal with different mud/debris flows. In combination with its dam-break modeling capability, the mud/debris flow enhanced FLDWAV model provides a useful tool in modeling landslide-induced mud/debris flows or those emanating from the dam-break-failure of tailings/debris dams.

MODEL FORMULATION

The one-dimensional Saint-Venant unsteady flow equations can be applied to non-Newtonian mud/debris flows by including an additional friction slope term (S_f) the conservation of momentum equation to account for the unique frictional resistance effects of the mud/debris solid-liquid mixture. The conservation equations of mass and momentum used in the FLDWAV model are:

$$\frac{\partial Q}{\partial x}+\frac{\partial(A+A_0)}{\partial t}-q=0 \tag{1}$$

$$\frac{\partial Q}{\partial t}+\frac{\partial(\beta Q^2/A)}{\partial x}+gA(\frac{\partial h}{\partial x}+S_f+S_e+S_i)+L+W_f B=0 \tag{2}$$

in which t is time, x is distance along the longitudinal axis of the channel, h is the water-surface elevation, A is the active cross-sectional area of flow, A_0 is the inactive (off-channel storage) cross-sectional area of flow, q is the lateral inflow or outflow, β is the coefficient for nonuniform velocity distribution within the cross section, g is the gravity constant, S_f is the friction slope due to boundary turbulent shear stress and determined by Manning's equation, S_e is the slope due to local severe expansion-contraction effects (large eddy loss), S_i is the friction slope associated with internal viscous dissipation and contact friction and collision of sediment clasts of non-Newtonian mud/debris fluid mixtures, L is the momentum effect of lateral flow, W_f is the wind term, and B is the channel flow width.

As previously mentioned, the resistance mechanism is different for different mud/debris flow states. The following three techniques can be used to determine the additional friction slope term (S_i) in Eq.(2), for different situations:

Viscoplastic technique

For the mudflow situation whose resistance behavior is mainly contributed by the internal viscosity and yield shear of the mud solid-liquid mixture, the viscoplastic technique can be used. The flow is assumed to be homogenous and viscous; the flow friction mainly depends on the flow's apparent viscosity (μ) and the sediment-water mixture's yield shear strength (τ_y). The friction slope (S_i) can be determined by applying an appropriate rheological equation describing a relationship between internal shear stress and shear-rate of non-Newtonian fluids. The resulting equation for the friction slope is generally a function of these parameters, as well as the flow state variables, h and Q.

Most mud/debris unsteady flow models have been based on viscoplastic techniques, such as the generalized voscoplastic fluid (GVF) model (Chen, 1988), the quadratic rheological model (Juien and O'Brien, 1993). In FLDWAV, the mud/debris friction slope (S_i) is derived based on the generalized power-law equation of an extended Bingham and Coulomb-viscous fluid model, i.e.,

$$\tau=\gamma S_i(y-z)=\tau_y+\mu(\frac{du}{dz})^{\eta} \tag{3}$$

in which τ is the internal shear stress, γ is the fluid mixture's unit weight, z is the distance from channel bed and y is the depth of the flow, u=u(z) is the longitudinal velocity in the x direction, η is an exponent of the power-law component of the shear stress (a Bingham fluid ($\eta=1$) is a commonly used assumption). Equation (3) can be solved for the depth mean velocity $V=f(y,\tau_y, \mu, \eta, S_i)$ by integrating z over

the flow depth (y) and assuming a parabolic velocity distribution in combination with a uniform velocity for $y \geq z \geq y-\tau_y/(\gamma S_i)$. This derivation results in a complicated implicit expression for the velocity (V) and friction slope (S_i) which does not lend itself for unsteady flow routing purposes. Instead, the following alternative semi-empirical equation which produces a closely approximate solution to Eq.(3) was proposed by the authors (Jin and Fread, 1997):

$$V=\frac{(0.74+0.656m)}{(m+1)(m+2)}\left(\frac{\tau_y}{\mu}\right)^m D\left(\frac{D}{D_0}-1\right)^{m+0.15} \tag{4}$$

in which $m=1/\eta$ and $m=1$ represents a Bingham fluid, D is the hydraulic depth, and $D_0=\tau_y/(\gamma S_i)$ can be regarded as the minimum depth for the mud/debris mixture to overcome the yield shear strength and begin to move. The following equation for S_i is derived from Eq.(4):

$$S_i=\frac{\tau_y}{\gamma D}\left[1+\left(\frac{(m+1)(m+2)Q}{(0.74+0.656m)(\tau_y/\mu)^m DA}\right)^{\frac{1}{m+0.15}}\right] \tag{5}$$

Equations (1) and (2), together with Eq.(5) for S_i are solved numerically with appropriate external (upstream/downstream) and internal (dam/bridge etc) boundary conditions. One of the characteristics of the viscous mud/debris flow is that the flow usually has relatively small velocities and large depths which are necessary to overcome the yield shear stress (τ_y) and sustain the motion on flat slopes; the initial water depths and the water depths beyond this mud/debris flow region are much smaller compared with the mudflow depths. There are many cases, also, where the mud/debris mixture moves over an initially dry or nearly dry channel and often has a steep-fronted leading edge associated with the mud/debris flood wave. For this situation, a wave-front tracking technique (Jin and Fread, 1997) tracks the moving wave front using a moving computational downstream boundary; the boundary is represented by an automatically generated Q=f(y) loop rating. Continuous relocation of the moving downstream boundary is accomplished by checking, at every time step, the mud/debris flow volume passed from the current boundary $x=x_j$ with the minimum volume for a steep front-edged wave to move between x_j and x_{j+1}. Extensive tests show that this technique is excellent in simulating moving steep-fronted waves of mud/debris flows from a zero (dry bed) or a very small initial flow condition.

In a previous study (Jin and Fread, 1997), the use of Eq.(5) was compared with two similar equations which are also based on viscoplastic modeling principles and model sensitivity studies were performed. The study indicated that Eq.(5) produced better and more stable/robust computational results when compared with some observed field data.

Granular sliding modeling technique

For mud/debris flows in which highly concentrated solid-liquid mixture slides

frictionally along relatively steep slopping channels, the flow moves downstream with high velocity as a heterogeneous surge with a steep, coarser-sediment flow front and more-fluid body behind the front. The highly frictional wave front acts much like a moving dam and the low-friction flow body pushes the resisting front from behind. The flow resistance behavior of this mud/debris flow is very much different from that of viscous mud/debris flows because the shear stresses are contributed by a combination of internal grain-contact friction, bed friction, and pore-fluid viscosity in which the grain-contact friction plays a dominant role. An appropriate resistance technique based this type of physics has been proposed by Iverson (Iverson, 1997).

Iverson analyzed data from large-scale experiments at the USGS debris-flow flume, and proposed a debris resistance formulation which he incorporated into a depth-averaged two-dimensional hydraulic numerical model. The friction slope due to the solid-liquid interactions and dynamic interactions between liquefied debris-flow body and high-friction debris-flow front was modeled by a specified longitudinal change of pore-pressure and local deformation of the flow. This technique is adapted in the FLDWAV model and the debris related friction slope term is determined based on a generalized profile of the longitudinal distribution of the pore-pressure and re-derived formulation for the debris friction slope to apply to the cross-section-averaged one-dimensional Saint-Venant equations of the FLDWAV model. The equation for S_f used in the FLDWAV model can be written as follows:

$$S_i=(\cos\theta-\frac{p_{bed}}{\gamma y})\tan\phi_{bed}+K_{a/p}(\cos\theta\frac{\partial y}{\partial x}-\frac{1}{\gamma}\frac{\partial p_{bed}}{\partial x})+\frac{1}{\gamma}\frac{\partial p_{bed}}{\partial x}-\cos\theta\frac{\partial y}{\partial x} \qquad (6)$$

in which θ is the angle of channel bed slope, y is the flow depth, p_{bed} is the pore-fluid pressure at the base of the flow, ϕ_{bed} is the friction angle of the debris-flow sediment on the channel bed, $K_{a/p}$ is a constant depending upon whether the flow is locally extending ($\partial Q/\partial t>0$ and K_a is used) or compressing ($\partial Q/\partial t<0$ and K_p is used). Typical values of the parameters γ, ϕ_{bed}, K_a and K_p were provided by Iverson (Iverson, 1997), i.e., 2100 kg/m^3 , 30° , 1.01 and 2.9, respectively.

The pore-fluid pressure distribution, p_{bed} (x), as specified in this technique, is based on observations from experimental data that show pore-fluid pressures are nearly zero in the debris surge front and gradually rise to levels nearly sufficient to liquefy the sediment in the body of debris flow; pore pressures then remain elevated until post-depositional sediment consolidation occurs. In the FLDWAV model, the following equation is used to specify the longitudinal pore-pressure distribution:

$$p_{bed}(x) = \gamma y\cos\theta\ [1-(\frac{x-x_1}{x_2-x_1})^e] \qquad (7)$$

in which x_2 is the x-location of the edge of the moving debris wave front, x_1 is the x-location of the end of the pore-pressure recovery (from zero to hydrostatistic value) region. This region (x_2-x_1) was assumed to extend about 35% of the debris flow length in Iverson's model. The parameter e in Eq.(7) specifies the pattern of the pore-pressure recovery, a value of e=1 assumes a linear distribution, as used by Iverson. The computational results have shown little sensitivity to this assumed length of the pore-pressure recovery region.

Although the pore-fluid pressure is not hydrostatic in the recovery region of (x_2-x_1) , a linear distribution along the flow depth (y) is assumed, which warrants the applicability of the Saint-Venant equations.

Using Eq.(7), the debris friction slope (S_i) of Eq.(6) can be derived:

$$S_i = y\cos\theta\left(\frac{x-x_1}{x_2-x_1}\right)^e \left[\frac{\tan\phi_{bed}}{y}+(K_{a/p}-1)\left(\frac{e}{x-x_1}+\frac{1}{y}\frac{\partial y}{\partial x}\right)\right] \qquad (8)$$

Combined resistance coefficient (pseudo Manning's n) technique

The physically-based viscoplastic technique and the granular sliding technique are useful and mostly accurate when accurate pre-determined parameters are available for describing the mud/debris flow characteristics such as τ_y, μ, γ and η in the viscoplastic technique, Eq.(4), and ϕ_{bed} and $K_{a/p}$ in the granular sliding technique, Eq.(7). The difficulties and uncertainties in determining these parameters in many situations promote the use of a simpler technique, i.e., a combined resistance coefficient technique. This technique lumps the mud/debris flow rheology and resistance into a single bulk resistance coefficient which is similar to the formulation in determining the channel turbulent shear friction slope (S_f) by Manning's equation for pure water flow or mudflood flow. Thus the mud/debris friction slope can be determined using the Manning equation and a pseudo Manning's n, i.e.,

$$S_i = \frac{n_i^2 Q^2}{\lambda A^2 R^{4/3}} \qquad (9)$$

in which n_i is the pseudo Manning'n for the mud/debris resistance, λ is a coefficient for different system of units (λ=1 for metric system and λ=2.21 for English system), R is hydraulic radius. Compared with typical values of 0.02 to 0.05 of the Manning's n for most turbulent channel water flows, typical n_i values can vary between 0.10 to 0.14 for debris flows.

In a recent application of the pseudo Manning's n method (Costa,1997), it was found that using this technique in the NWS DAMBRK flood routing model closely replicated field-documented stages of historic lahars from Mt.Rainier, Washington,

and Mt. Hood, Oregon. Modeled time-of-travel of the lahars debris waves were generally consistent with documented lahar travel-times from many other volcanoes around the World.

The pseudo Manning's n technique is not physically based and has its fundamental weakness because the physical mechanisms involved in the frictional energy dissipation of mud/debris flows are significantly different from those associated with turbulent pure water flows for which the Manning's equation is well established. Albeit this limitation, the pseudo Manning's n technique is still useful for its simplicity and lack of requirement for the mud/debris related parameters. It can be used in any dynamic routing model without modification to the model to provide a first order estimation of mud/debris unsteady flows.

Limitations of the mud/debris flow friction techniques

It is worthwhile to examine the application limitations of these three mud/debris resistance modeling techniques.

Generally, the viscoplastic technique can be applied to mud/debris flows in channels with mild slopes, while the granular sliding technique is used for the highly concentrated mud/debris flows in channels with steep slopes. Hence, a factor in determining the applicable mud/debris resistance technique is the concentration of the solid-liquid mixture. The concentrations by volume of 0.2, 0.40 and 0.50 can be used as a rough criterion for classifying among mud floods, mudflows and debris flows, respectively. A concentration by volume of less than 0.2 is regarded as water flood. The volume fraction of solid grains typically ranges from about 0.2 to 0.4 for mud floods and 0.4 to 0.5 for mudflows. The viscoplastic technique can be used for some mud floods and for mudflows. A larger concentration by volume is usually associated with the debris flows, where the granular sliding technique can be used.

Another factor to consider is the channel slope, which can provide an approximate guide for the applicability of the viscoplastic and granular sliding techniques. For the granular sliding debris flows, the wave front can be assumed to move like a kinematic wave. The total friction slope approaches the channel bed slope for a kinematic-type flow. If the turbulent shear friction slope is neglected and $K_a = 1.0$ is used in Eq.(8) for an extending flow and $(x-x_1)/(x_2-x_1) \approx 1$ for the wave front region, the following relation can be obtained:

$$S_0 = \cos\theta \tan\phi_{bed} \qquad (10)$$

Recognizing that $S_0 = \sin\theta$ is the channel bed slope, Eq.(10) can be used to show that $\theta = \phi_{bed}$ under these assumptions. Therefore a steep slope of $\theta \geq \phi_{bed}$ is appropriate for the use of the granular sliding technique, while the viscoplastic technique is used for channels of smaller θ. A typical value of ϕ_{bed} is between 20° to 30°.

The combined resistance coefficient technique, on the other hand, seems to have no limitations as long as an appropriate pseudo Manning'n can be selected. It is

also beneficial to examine the relative importance in Eq.(2) of the friction slope due to the turbulent shear stress (S_f) compared with the mud/debris friction slope (S_e) for mud/debris flows. The turbulent shear friction slope (S_f) can be compared with the mud/debris friction slope (S_i) by using the pseudo Manning'n technique as an approximation for any of the three mud/debris flow friction techniques. Thus, it can be obtained that $S_f/S_i=(n/n_i)^2$. Using this ratio, it can be concluded that the effects of the turbulent shear friction slope is negligible only for situations when the pseudo Manning,s n is much larger than the boundary Manning's n. For example, if values for n and n_i are 0.03 and 0.13, the ratio $S_f/S_i=0.053$ which means that the turbulent friction of the boundary roughness is negligible. In real applications, one only need to specify a combined Manning's n to represent both turbulent shear friction and mud/debris shear friction.

APPLICATION CASE STUDIES

Case 1. Anhui debris dam failure flood

The dam containing the contents of the Jinshan tailings debris reservoir in Anhui, China, breached in the early morning of April 30, 1986 (Han and Wang, 1996). The dam-break induced mud/debris flood engulfed a village about 0.75 km downstream of the reservoir; all of the village residents were killed in the disaster. Measurements of the inundation area were made after the debris/mud flooding event.

Han and Wang (1996) simulated the unsteady mud/debris flow using a two-dimensional, depth-averaged model with a 3-D rheological stress and strain equation similar to the viscoplastic modeling technique reported in this paper. An assumed inflow hydrograph was used as the upstream boundary condition. The FLDWAV model is applied to this case using the three different resistance techniques. The following data provided by Han and Wang is used in the mud/debris enhanced one-dimensional FLDWAV model to simulate the breaching of the dam and traveling of the dam-break induced debris/mud flow: total volume of water-debris mixture in the reservoir is about 8.45×10^5 m^3; top width of the reservoir at the dam is 245 m and height of the dam is 21.7 m; and the dam-break induced flow lasted less than 5 minutes. The final rectangular-shaped dam-breach width is 240m and a 1 minute time for breach failure is used in the FLDWAV model to simulate the dam-breach outflow hydrograph. It is assumed that downstream cross-sections are irregular trapezoids with an average width of 210m to 580m and a channel bottom slope from about 0.0109 (0.62°) upstream to 0.00076 (0.043°) downstream. The following Bingham fluid properties are used for the viscoplastic technique: $\mu=2.1$ N s/m^2 (0.044 lb s/ft^2), $\tau_y=38$ N/m^2 (0.80 lb/ft^2), and $\gamma=15700$ N/m^3 (100 lb/ft^3). For the pseudo Manning's n technique, values of the pseudo Manning's n are specified as $n_i=0.05$ for nearly zero low flow and $n_i=0.11$ for the peak flow. Since the initial flow is almost zero, the wave-front tracking option in FLDWAV is used for the viscoplastic technique.

Figure 1 compares the computed peak discharge profiles and wave travel times using the viscoplastic and pseudo Manning's n techniques to determine the mud/debris friction slope. The granular sliding technique is not shown since it was not numerically stable in this case because of the flat channel slope, i.e., $\theta < 1°$ and $\theta < \phi_{bed}$. The viscoplastic technique produces an excellent total wave progression (inundation) distance of the waste mud/debris flow compared with the post-event observation of inundation distance. Unlike the viscoplastic technique in which the flow finally stopped because the moving mixture's momentum has decreased to such a small value that it is unable to overcome the mixture's internal yield shear stress, the pseudo Manning's n technique dose not produce a final stopping point of the flow. However, it does produce a reasonable attenuation of the dam-break induced mud/debris wave up to the observed inundation limit of the mud/debris flow.

Figure 2 shows the computed discharge hydrographs at three locations along the reach (x=0 at dam site, x=400m, and x=800m) from the two techniques. One characteristic feature simulated by the viscoplastic technique is that the mud/debris wave moves with a steep front and both the discharge and stage hydrographs reach their peak very quickly. This, along with the greater density of mud/debris floods compared to water floods, contributes to the fact that even a small mud/debris flood can cause devastating damage in life and property as occurred in this case. The pseudo Manning's n technique tends to smear the sharpness of the wave as it moves downstream.

Figure 3 shows computed mud/debris surface profiles at t=0.005, 0.01, 0.02, 0.05 and 0.09 hours from both the viscoplastic technique and the pseudo Manning's n technique. The dam breaching started at t=0.0 due to an assumed overtopping failure and reached its final shape within the assumed 1 minute time of failure, and the mud/debris mixture wave front propagated downstream to a final inundation limit within a total time of about 5 minutes. This agreed with the site report that the flooding lasted less than 5 minutes. The computed inundation distance of 1200m by the viscoplastic technique compares well with the observed inundation distance of about 1210m.

Some sensitivity tests are performed to examine the effects of the mud/debris related parameters to the computational results. For the viscoplastic technique, the combinations of different μ and τ_y values (recommended values as mentioned above, 20-25% increased values and 20-25% decreased values) are grouped and tested. It is found that the biggest percentage changes occurred in the computed wave travel times as μ and τ_y are both increased or decreased. An 20% increase or 20% decrease in the values of μ and τ_y caused less than 10% of the overall differences in the computed wave travel times, while a maximum of 15% difference occurred near the computed inundation limit. Similar results are also found for the sensitivities of the pseudo Manning's n. A change of 25% in the value of the pseudo Manning's n resulted in an maximum 17% of difference in the computed wave travel times.

Case 2. USGS debris-flow flume experiment data

One case study from the U.S. Geological Survey (USGS) large-scale debris-flow flume experiments is used to test the mud/debris enhanced FLDWAV model. The flume is a reinforced concrete channel with a length of about 80m, a width of 2m, and a depth of 1.2m. The slope of the flume channel is 0.515 (31 degree) and the flume base empties into a wide area with a nearly horizontal concrete surface . A 9.4 m^3 heap of sediment was saturated and the debris mixture of water-saturated sand and gravel was suddenly released from a gate at the head of the flume within about 1 second. Based on this condition, a discharge hydrograph is established as the upstream boundary condition for the computation. Detailed flow measurements were made at the cross sections located 2m, 33m and 67m downstream of the head gate.

This is a typical debris flow case in which a highly concentrated mud/debris mixture (the concentration by volume is about 0.6) travels along a very steep channel. The granular sliding and pseudo Manning'n techniques are both tested in this case. Values of the parameters used in the granular sliding technique are $\theta=31°$ and $\phi_{bed}=30°$. For the pseudo Manning's n technique, it was found that use of a single value of the pseudo Manning's n applications does not produce reasonable results. Similar to river flood modeling applications, expressing the Manning's n as a function of local discharge produced good results. In this test, the pseudo Manning's n is specified as $n_i=0.02$ for nearly zero base flow and $n_i=0.09$ for the peak discharge, with linear interpolation used for all intermediate flows.

Figure 4 compares the computational results from these two techniques with the observed data for stage hydrographs at three locations, x=2m, 33m and 67m. Both techniques predict reasonably well the travel time of the advancing debris wave and the overall shape of the debris flow surge.

Another interesting test is to examine the model's capability to predict the runout of the debris flow. In this case, the flat open area at the end of the flume acted like a debris fan. The runout surface is modeled by extending the steep flume channel of 2m wide to a nearly flat gradually expanded channel of about 12m wide at x=120m. When applied to this extended channel, the two techniques were unable to predict an exact stopping point of the debris runout, but both techniques very well predicted an accelerated attenuation in the debris fan or runout surface area, as shown in Figure 5. If an inundation limit is assumed to be where the flow has attenuated to at least 5% of the upstream peak flow, it can be reasonably specified at about x=100-110m. This compares well with the observed inundation limit of x=99m. The experimental flow required about 11 s to reach its inundation limit, whereas the FLDWAV model using both the granular sliding and the pseudo Manning's n techniques predicted that about 13 s would be required to reach the point of the runout limit at x=100m.

Some tests are done regarding the model sensitivities to the mud/debris related parameters. Values of $\phi_{bed}=25°$ and $\phi_{bed}=20°$ are also tested and the computational results are compared with those of using $\phi_{bed}=30°$. This 15-33% decrease in ϕ_{bed} resulted in less than 12% of the differences observed in computed wave travel time, depth and discharge. On the other hand, a 30% increase or decrease of the pseudo

Manning's n were found to cause about 20% differences in the computational results in the pseudo Manning's n technique.

As experienced in this case, one of the characteristic features of most mud/debris flows is that the flow regime can be supercritical ($V>\sqrt{gD}$) due to the high velocity of the debris mixture flow in a very steep channel, while a subcritical regime ($V<\sqrt{gD}$) exists in the rapidly decelerated flow region in the debris fan or runout area. The supercritical-subcritical-mixed flows can be modeled in FLDWAV by either the LPI (Local Partial Inertial modification) enhanced implicit solution scheme (Fread, et al. 1996) or a characteristic-based upwind explicit solution scheme (Jin and Fread, 1997).

Case 3. Aberfan coal waste dump failure

The Aberfan mud/debris flow disaster occurred in Wales in 1965. In this case, waste material from a 37 m high dump from a coal-mining operation liquefied and flowed down a slope of about 12° (S_0 =0.208) over a distance of about 600 m until it inundated a school and other buildings located in the flow path. One hundred and twenty lives were lost in the buried portion of the school building. This case was investigated by using an analytical mudflow simulation technique based on a laminar Bingham fluid model (Jeyapalan, et al. 1983). The FLDWAV model is also applied to this event by simulating it as a dam-break induced mud/debris flow case. The downstream channel has triangular cross sections with a side slope of about 1 vertical to 2 horizontal. A hypothetical waste reservoir is placed at the upstream end, and the dam is breached at the beginning of routing. The final breach shape is assumed to be the same as the triangular channel cross-sections and a time of failure of about 1 minute is used to simulate the dam-failure hydrograph.

All three resistance techniques of the FLDWAV model are applied to this case and they are found to produce similar computational results. For the viscoplastic technique, according to Jeyapalan, et. al (1993), the following mud/debris fluid mixture properties are used: μ=958 N s/m^2 (20 lb s/ft^2), τ_y =4794 N/m^2 (102 lb/ft^2), and γ=17640 N/m^3 (112 lb/ft^3). For the pseudo Manning's n technique, the Manning's n is also specified as a function of flow discharge with 0.05 for nearly zero low flow and 0.12 for the peak flow. For the granular sliding technique, it is found that a value of ϕ_{bed}=10° produced stable computational result.

Figure 6 shows the computed dam-break induced mud/debris wave travel times for each of the three techniques. An observed data point is also shown. In this case, the mud/debris flood was observed to reach the school building at about x=600m within about 120s. The computed travel times for the three techniques range from about 120s to 140s. Figure 7 compares the computed flow depth hydrographs at x=600m. It can be seen that the peak flow depth can be as high as 9m at this location. Such a large, fast moving sharp wave can explain the devastating damages inflicted upon the school and its occupants.

Case 4. Rudd Creek landslide-induced mudflow

A mud/debris flow occurred in 1983 at Davis County, Utah. The flow was initiated by a landslide in which approximately 64,000 m^3 of hill solid material was liquified, collapsed, flowed down the hill and submerged a residential block just downstream of the landslide. This case has been successfully simulated by using a two-dimensional unsteady debris flow model (O'Brien, Julien, and Fullerton,1993). The FLDWAV model is applied to this case to test: (1) using the dam-break simulation capability to generate the landslide-induced hydrograph; (2) unsteady mud/debris flow routing using viscoplastic technique and pseudo Manning's n technique and (3) model performance of simple one-dimensional treatment.

In this case, the landslide mud/debris mixture flowed along the hill slope and not in single channel. Although the phenomena is two-dimensional, an one dimensional approximation can be made by setting a nonprismatic channel according to the possible flow paths from topological map (Jin and Fread 1997). The channel has a slope of about 6° (S_0=0.105) at the apex of the channel and about 0.5° (S_0=0.0087) at end of the debris fan, and the channel widths varies between 30m and 230m. In order to generate the upstream landslide hydrograph at x=0 by dam-break simulation, a hypothetic 30m high dam is placed at upstream end with a 150 m of longitudinal runoff distance for its reservoir. The dam is assumed to have a breaching fail at the beginning (t=0.0) and totally failed within 6 minutes.

For viscoplastic technique, the mud/debris properties are estimated according to the value of about 0.5 of the concentration by volume of the mud/debris mixture and the empirical relationship (O'Brien and Julien, 1985). The following properties are used in the computation: μ=958 N s/m^2 (20 lb s/ft^2), τ_y =956 N/m^2 (20 lb/ft^2), γ=15750 N/m^3 (112 lb/ft^3), and n=0.05. For the pseudo Manning's n technique, various values of the Manning's n are tested and none of them produced reasonable flow attenuation, this suggests that the pseudo Manning's n technique is not suitable for simulating very viscous (μ>700 N s/m^2 , τ_y >700 N/m^2) mud/debris flow on channels with small slope (θ<5°).

Figure 8 shows the computed discharge hydrographs by viscoplastic technique at x=0 (landslide site), x=130 and x=250 m. The dotted line represents the landslide hydrograph proposed by the U.S. Army Corps of Engineers (Incorporating 1986), the FLDWAV dam-break-simulation generated a similar hydrograph with about same peak value but with a centroid shift toward to later time. Figure 9 shows the computed maximum flow depth profile and wave travel time, the computational traveling distance of x=350 m compares well with the observed inundation limit of about 360 m. The computed peak flow depths are about 3.5 m at upstream and about 0.9 m in the stopping point while the observed mudflow depths were 3.7 m and 0.6-0.9 m, respectively. The computed average wave speed is about 0.6 m/s while the eyewitness accounting for the speed was about 0.6-1.2 m/s. These results indicate that one-dimensional approximation can also produce good computational results.

Applicability of dynamic routing compared to kinematic routing

In some mudflow applications, the kinematic wave assumption was made for mud/debris unsteady flows so that a simple kinematic model could be used. The applicability and limitations of kinematic modeling as compared with fully dynamic modeling such as the FLDWAV model are briefly examined herein. Since the FLDWAV model gives numerical solutions based on the dynamic equations, these solutions can be used to evaluate the different terms in the complete one-dimensional momentum Eq.(2) of the Saint-Venant equations, and check how well the kinematic assumption is applicable for mud/debris flows by comparing the importance of the different terms.

The kinematic wave model is based on the assumption that the total friction slope S ($S=S_f+S_i+S_e$ in Eq.(2)) is equal to the channel bad slope (S_o), i.e, $S=S_o$. The applicability of this assumption to the 4 cases presented in this paper is checked. In each case, one x-location is chosen at the mid-point of each routing reach and the time-variation of the total friction slope is computed for the rising limb of the hydrograph and compared with the local channel slope by computing the slope ratio (S/S_o). Figure 10 shows the slope ratio as functions of the time normalized by the time-of-rise of each hydrograph (t_r) for each of the four cases. A value of 1.0 for the slope ratio indicates that the wave is purely kinematic and the degree of the departure from 1.0 measures the contribution of the inertial and pressure terms which are neglected in the kinematic assumption. The largest departure from 1.0 occurred in the case of Anhui debris dam in which S/S_o attains a value as high as 22.0, while the USGS debris flume flow and the Aberfan debris flow have less than about 5-10% departure for most of the rising limb. It can be seen from these results that the smaller the channel slope causes a more significant departure of the ratio from the kinematic assumption. Also, considering the fact that the important part in the mud/debris simulation is the debris fan region where the channel slope often becomes very flat, this region requires accurate simulation since it is often where developments and their occupants are located. Therefore, it can be seen from this study that the kinematic wave model should be used very cautiously in these situations, although there will be little computational difference between a dynamic model and a kinematic model in the steep sloping portions of mud/debris unsteady flow applications.

CONCLUSIONS

The open channel unsteady flow models based on the one-dimensional Saint-Venant unsteady flow equations can be applied to simulate non-Newtonian mud/debris flows if an additional friction slope (S_i) representing the internal viscous shear friction and the internal grain-contact friction is appropriately specified. The mud/debris unsteady flows can have distinct physical characteristics for different types of the mud/debris mixtures and channel bed slopes; therefore, different modeling techniques are needed in order to simulate the variety of mud/debris flows. The three techniques tested in this paper enhance the capability of the NWS FLDWAV dynamic flood routing model to simulate the mud/debris unsteady flows

when appropriately applied. The computational results in the Anhui dam-break and Aberfan dam-break case studies show that the viscoplastic technique which uses Eq.(5) for the mud/debris friction slope along with a wave-front tracking technique produced excellent computational results in modeling the mudflows. Comparison of the computed results utilizing the USGS large-scale experimental data shows that the granular sliding technique which uses Eq.(8) is capable of modeling the debris flows on steep slopes. The combined resistance coefficient (pseudo Manning's n) technique is found to be a very useful alternative for modeling both mud and debris flows if the data required to use the other techniques are not available. It is also found to be the most robust among the three techniques. The pseudo Manning's n technique, which uses Eq.(9), is suggested to be a function of the discharge, with a small n value (0.03-0.06) for low flows and a large n value (0.08-0.16) for near peak or peak flows. However, this technique is not capable of predicting a final inundation distance. The inundation distance can be estimated in this technique by allocating a point where the flow attenuation has reached a value of less than 5% of the upstream peak flow. Dynamic routing is recommended over the more simple kinematic routing when the routing reach is not steep (say $S_0 < 4°$).

APPENDIX I. REFERENCES

Chen, C.L. (1983). "On frontier between rheology and mudflow mechanics." in *Frontiers in Hydraulic Engineering*, Edited by Shen, H.T., ASCE, New York, 113-118.

Chen, Cheng-lung and Ling Chi-hai, (1997). "Resistance formulas in hydraulic-based models for routing debris flows", in *Debris-Flow Hazards Mitigation: Mechanics, Prediction, and Assessment*, Edited by Cheng-lung Chen, ASCE, New York, 360-372.

Costa, J.E. (1997). "Hydraulic modeling for lahar hazards at cascades volcanoes", Environmental & Engineering Geoscience, Vol. III, No.1, 21-30.

Fread, D.L. (1993). Chpt 10: Flow routing, in *Handbook of Hydrology* , Edited by Maidment,D.R., McGraw-Hill, New York, 10.1-10.36

Fread, D.L. (1988). The NWS DAMBRK model: Theoretical background and user documentation, HRL-258, Hydrological Research Laboratory, National Weather Service, Silver Spring, Maryland 20910.

Fread, D.L., Jin, M., and Lewis J.M., (1996). "An LPI numerical implicit solution for unsteady mixed-flow simulation", in *Proc. of North American Water and Environment Congress*, CD-ROM published by ASCE.

Han,G., and Wang,D. (1996). "Numerical modeling of Anhui debris flow." *J. Hydraulic Eng.*, ASCE, 122(5), 262-265.

Incorporating the effects of mudflows into flood studies on alluvial fans. (1986). U.S. Army Corps of Engineeers, Omaha District, Omaha, Ne.

Iverson, R.M. (1997). "The physics of debris flows", Reviews of Geophysics, Vol.35, No.3, 245-296.

Iverson, R.M., (1997). "Hydraulic modeling of unsteady debris-flow surges with

solid-fluid interactions", in *Debris-Flow Hazards Mitigation: Mechanics, Prediction, and Assessment*, Edited by Cheng-lung Chen, ASCE, New York, 550-560.
Jeyapalan, J.K., Duncan, J.M., and Seed, H.B., (1983). "Analysis of flow failures of mine tailings dams", J. Geotechnical Eng., ASCE, 150-189.
Jin, M., and Fread, D.L. (1997). "One-dimensional routing of mud/debris flows using NWS FLDWAV model", in *Debris-Flow Hazards Mitigation: Mechanics, Prediction, and Assessment*, Edited by Cheng-lung Chen, ASCE, New York, 687-696.
Jin, M., and Fread, D.L. (1997). "Dynamic flood routing with explicit and implicit numerical solution schemes", *J. Hydraulic Eng.*, ASCE, 123(3), 166-173.
Julien, P.Y. and O'Brien, J.S., (1997). "On the importance of mud and debris flow rheology in structural design", in *Debris-Flow Hazards Mitigation: Mechanics, Prediction, and Assessment*, Edited by Cheng-lung Chen, ASCE, New York, 350-359.
O'Brien, J.S., Julien, P.Y., and Fullerton, W.T. (1993). "Two-dimensional water flood and mudflow simulation." *J. Hydraulic Eng.*, ASCE, 119(2), 244-261.
O'Brien, J.S., and Julien, P.Y. (1985). "Physical properties and mechanics of hyperconcentrated sediment flows." in *Delineation of Landslide, Flash Flood and Debris Flow Hazards in Utah* , UWRL/G-85/03, Utah Water Research Laboratory, Utah State University, 260-278.
Schamber, D.R., and MacArthur, R.C. (1985). "One-dimensional model for mud flows." in *Hydraulics and Hydrology in the Small Computer Age*, Vol.1, ASCE, 1334-1339.

APPENDIX II. NOTATION

The following symbols are used in this paper:

A = active cross-sectional area of flow;
A_o = inactive (off-channel storage) cross-sectional area of flow;
B = channel flow width;
D = hydraulic depth;
D_o = minimum depth of viscous mud/debris flow;
e = constant;
g = gravity constant;
h = water surface elevation;
L = momentum effect of lateral flow;
$K_{a/p}$ = constants;
x = distance along longitudinal axis of a channel;
m = constant;
n = Manning's n;
n_t = pseudo Manning's n for mud/debris flow;
p_{bed} = pore-fluid pressure;
q = lateral flow discharge;
Q = flow discharge;

R = hydraulic radius;
S_e = slope duo to local expansion-contraction effects;
S_f = channel boundary turbulent frictional slope;
S_f = mud/debris frictional slope;
S_o = channel bed slope;
t = time;
u = longitudinal velocity of the flow;
V = cross-sectional velocity of the flow;
x_1 = x-location of debris flow wave front;
x_2 = x-location of pore-pressure recovery;
y = water depth;
z = vertical distance from channel bed;
ϕ_{bed} = friction angle of debris flow sediment;
θ = channel bed slope in degree;
η = exponent of power-law for viscous shear stress;
β = velocity coefficient in momentum equation;
λ = coefficient for different units in Manning's equation;
γ = unit weight;
τ_y = yield shear strength;
μ = viscosity;

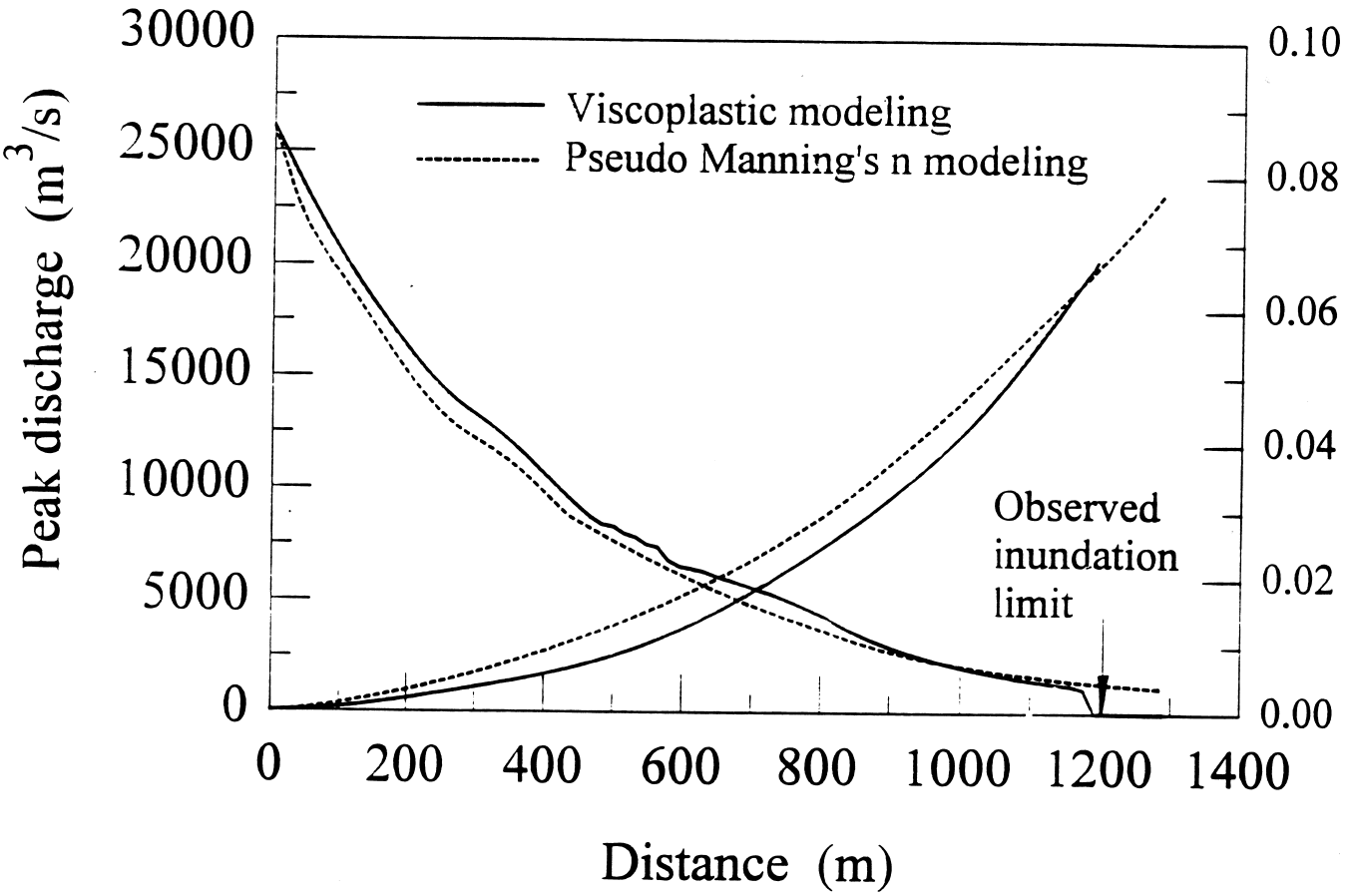

Figure 1 Peak discharges and wave travel times for Anhui dam

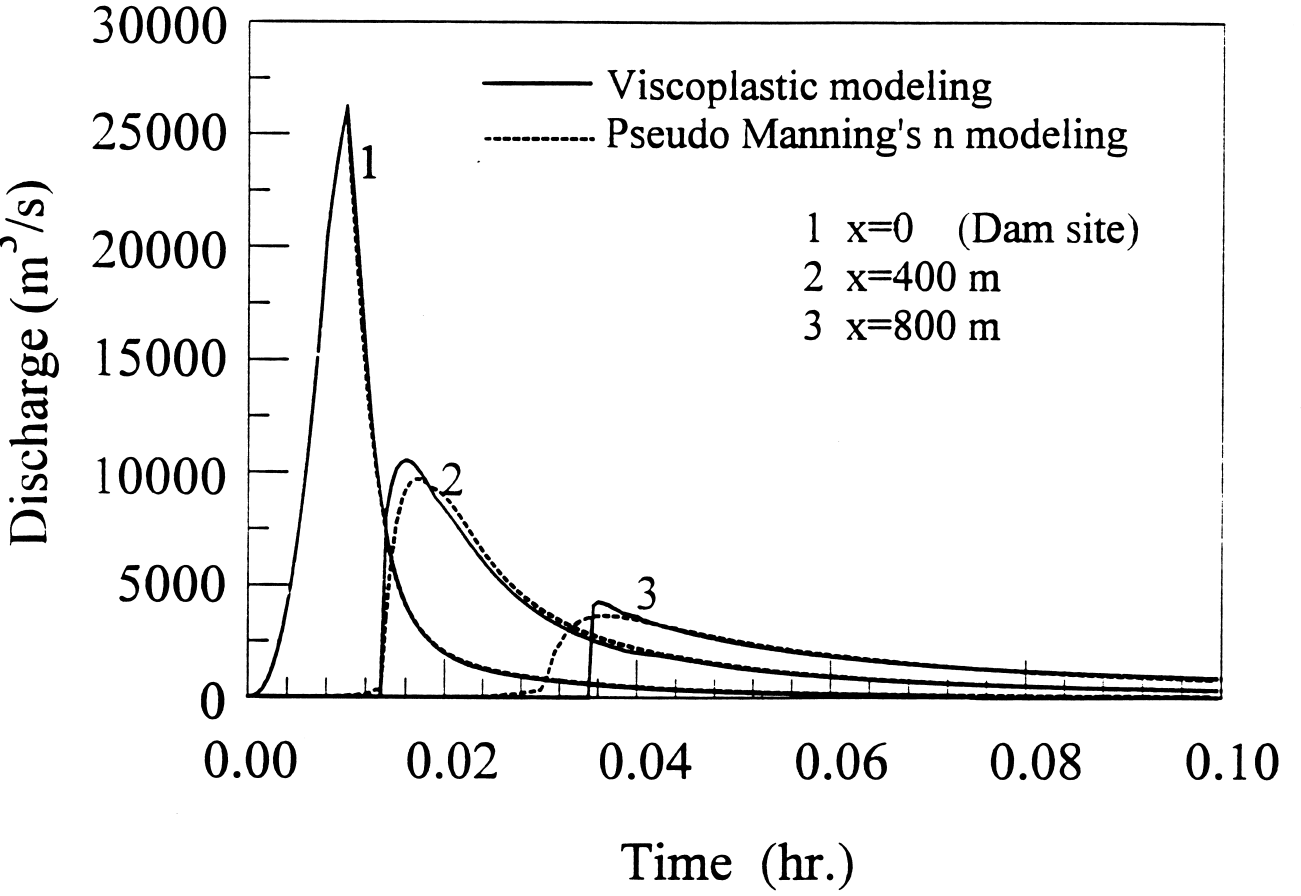

Figure 2 Computed hydrographs for Anhui dam

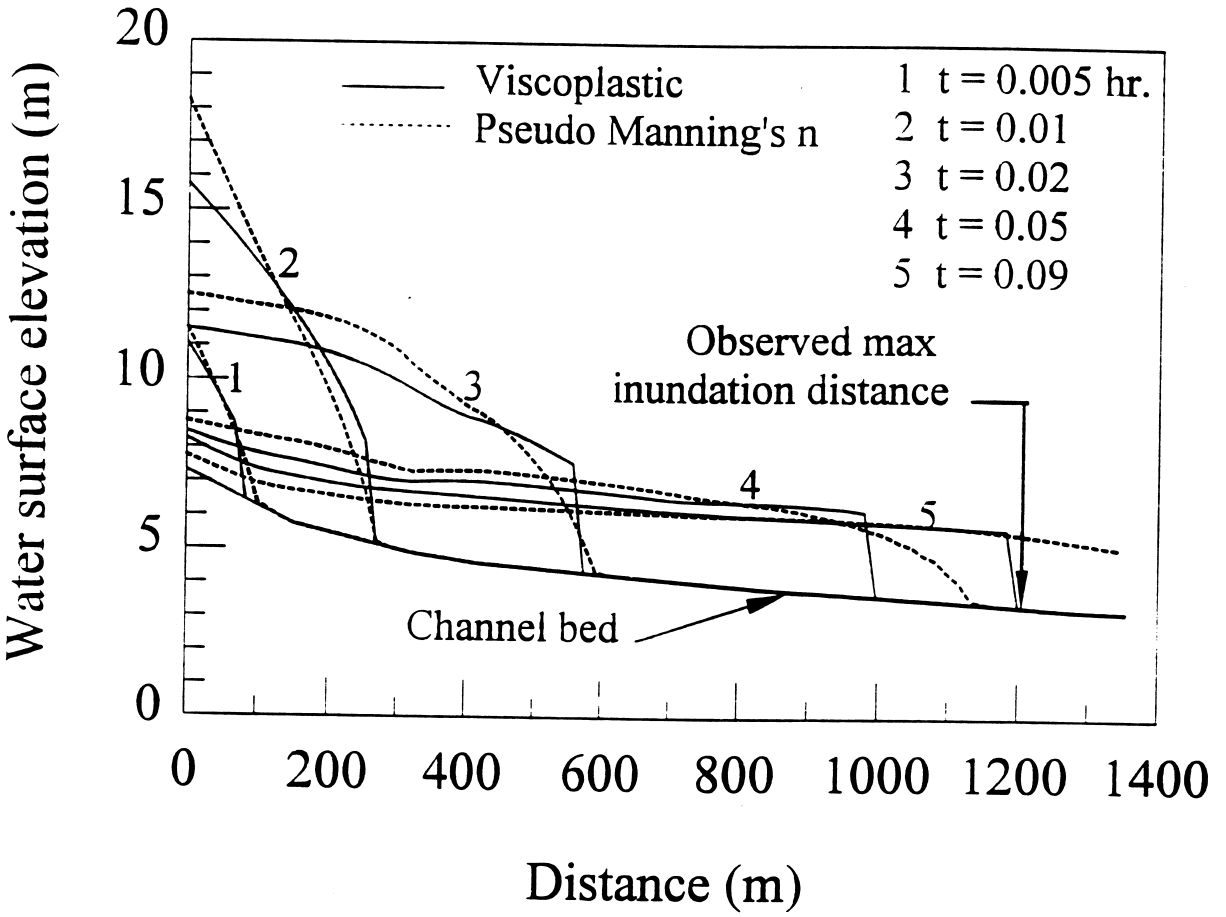

Figure 3 Computed water surface profiles for Anhui dam

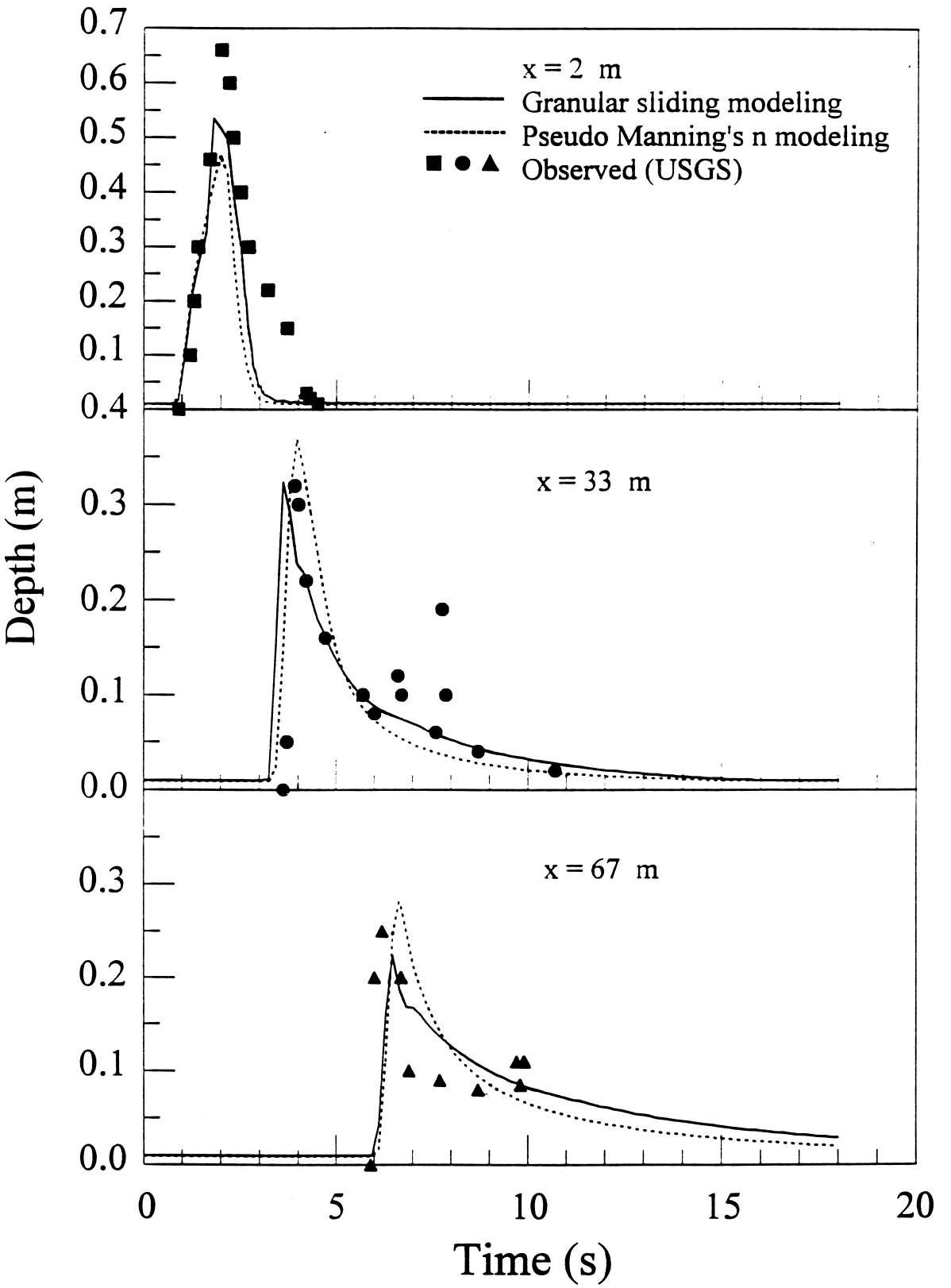

Figure 4 USGS Debris flume data testing

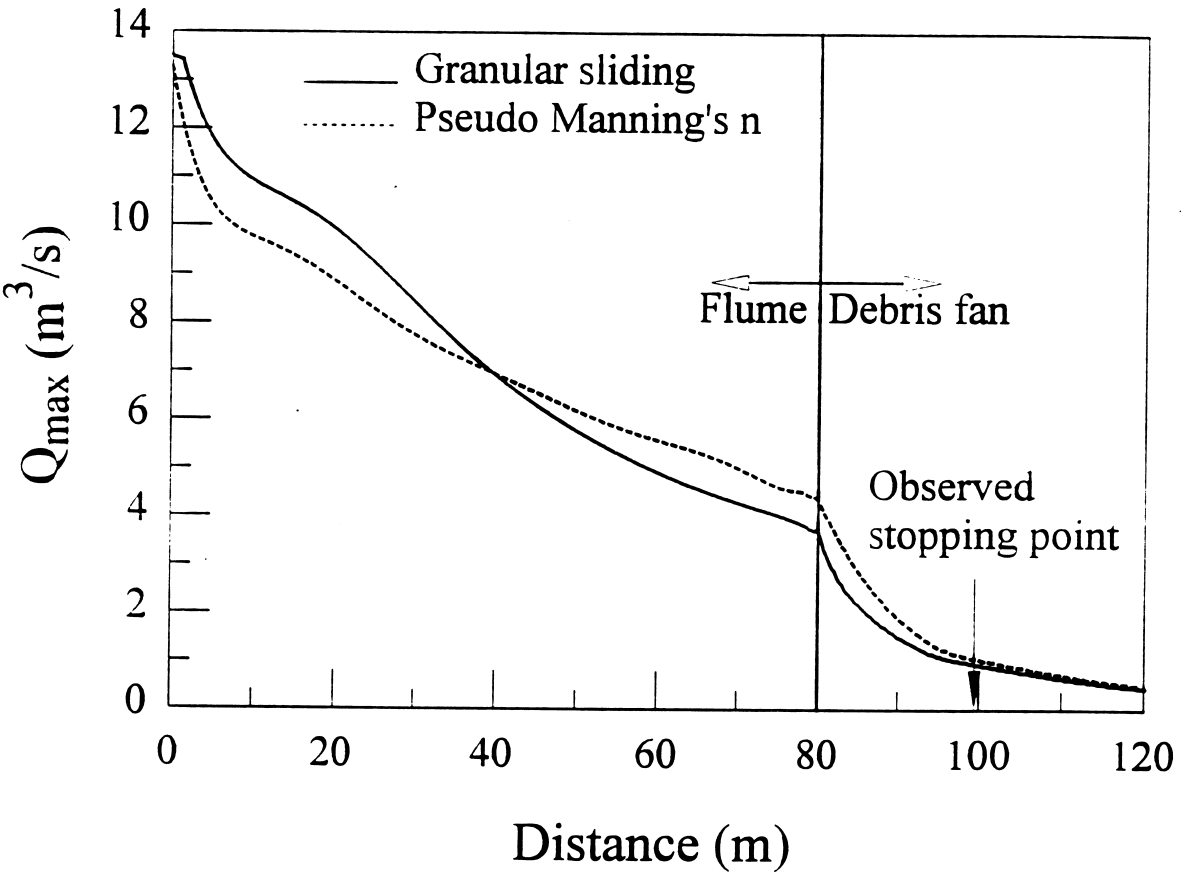

Figure 5 Peak discharge and wave travel time of USGS debris flow

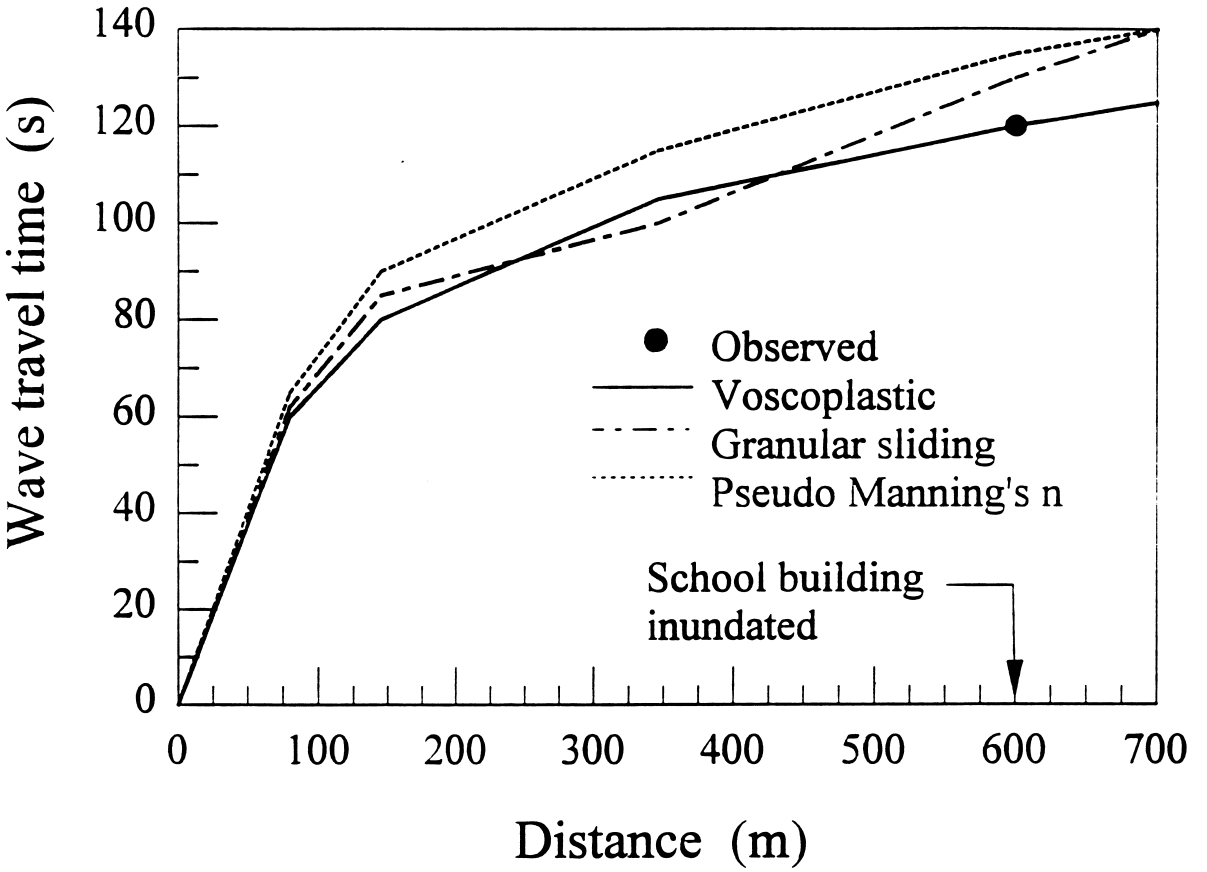

Figure 6 Wave travel times for Aberfan dam

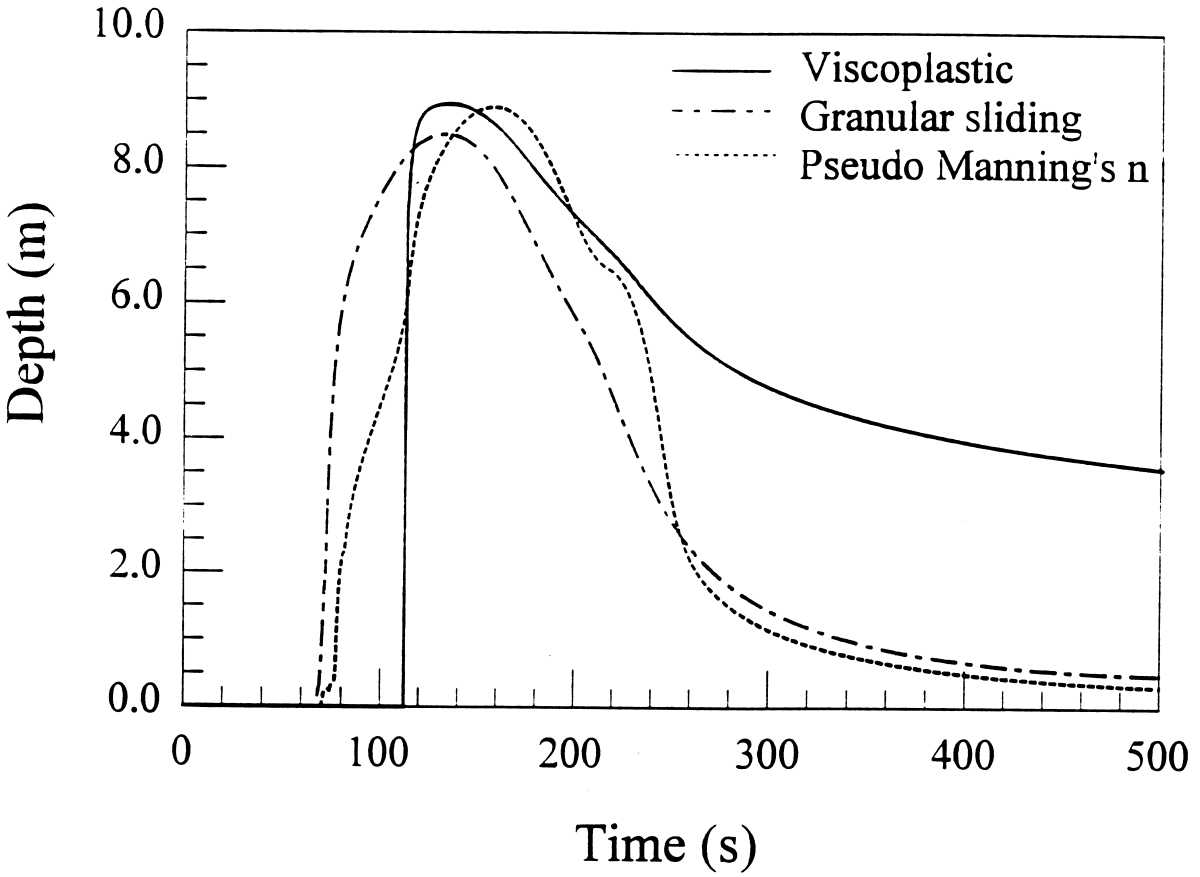

Figure 7 Computed depths at x=600 m from Aberfan dam

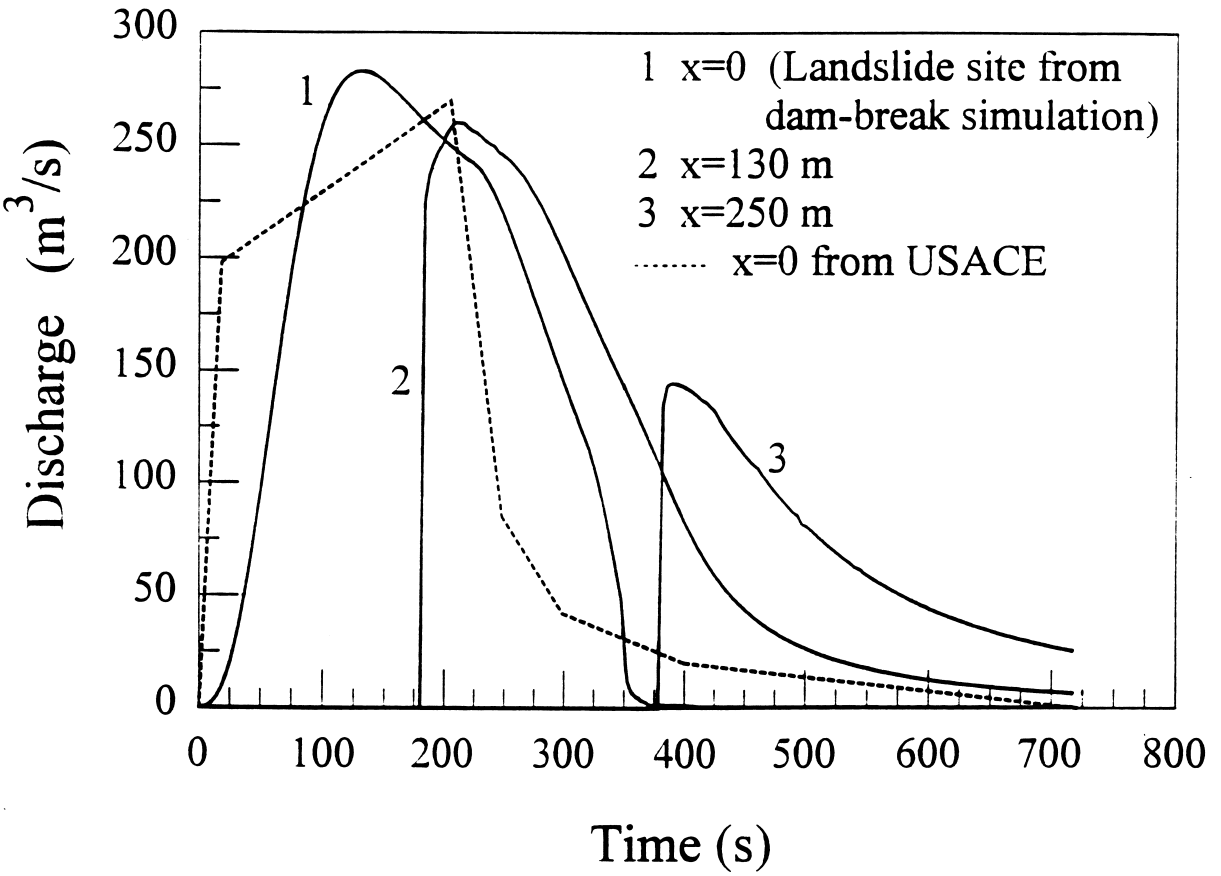

Figure 8 Computed discharge hydrographs for Rudd Creek

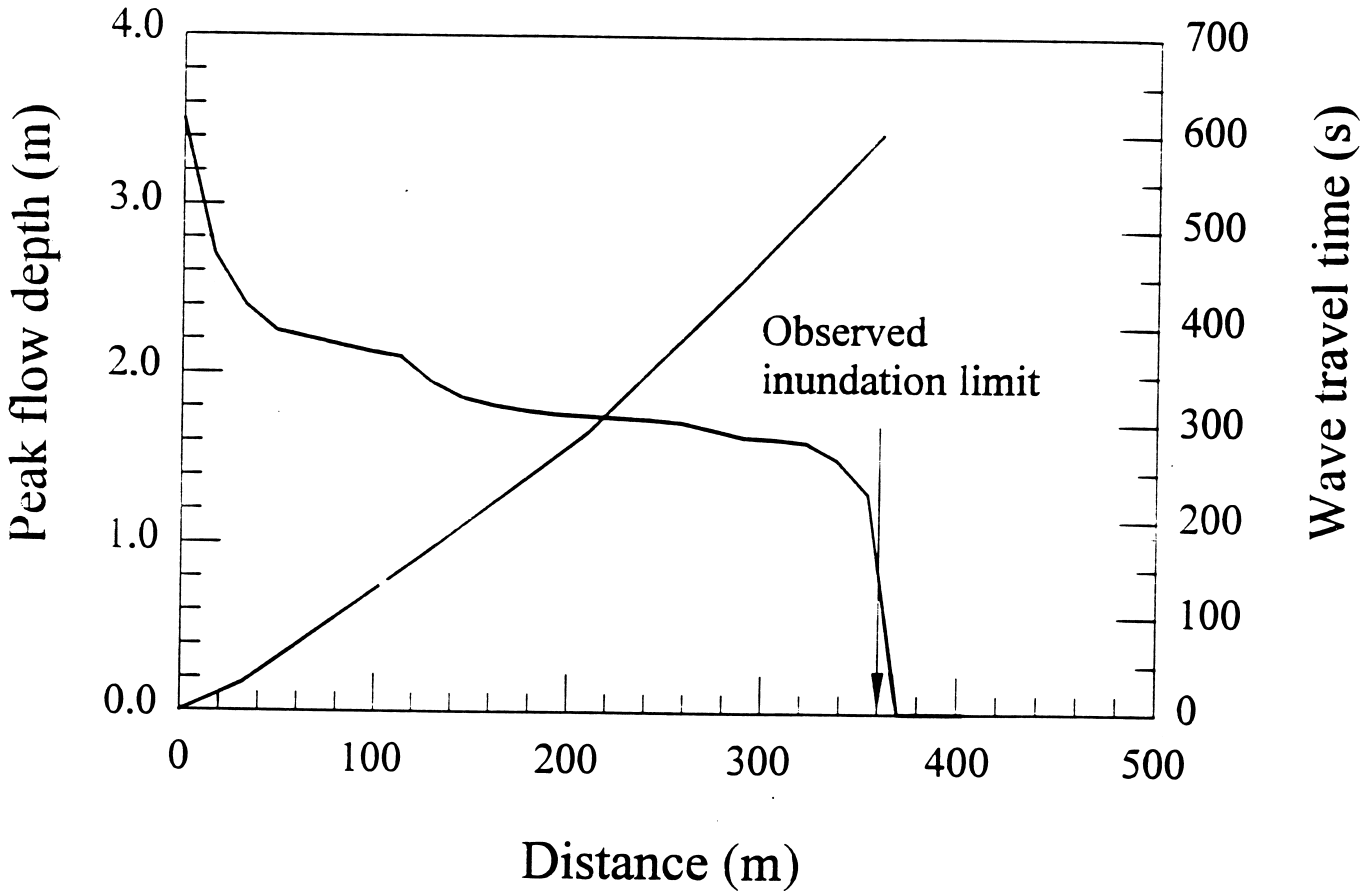

Figure 9 Peak flow depth and wave travel time for Rudd Creek

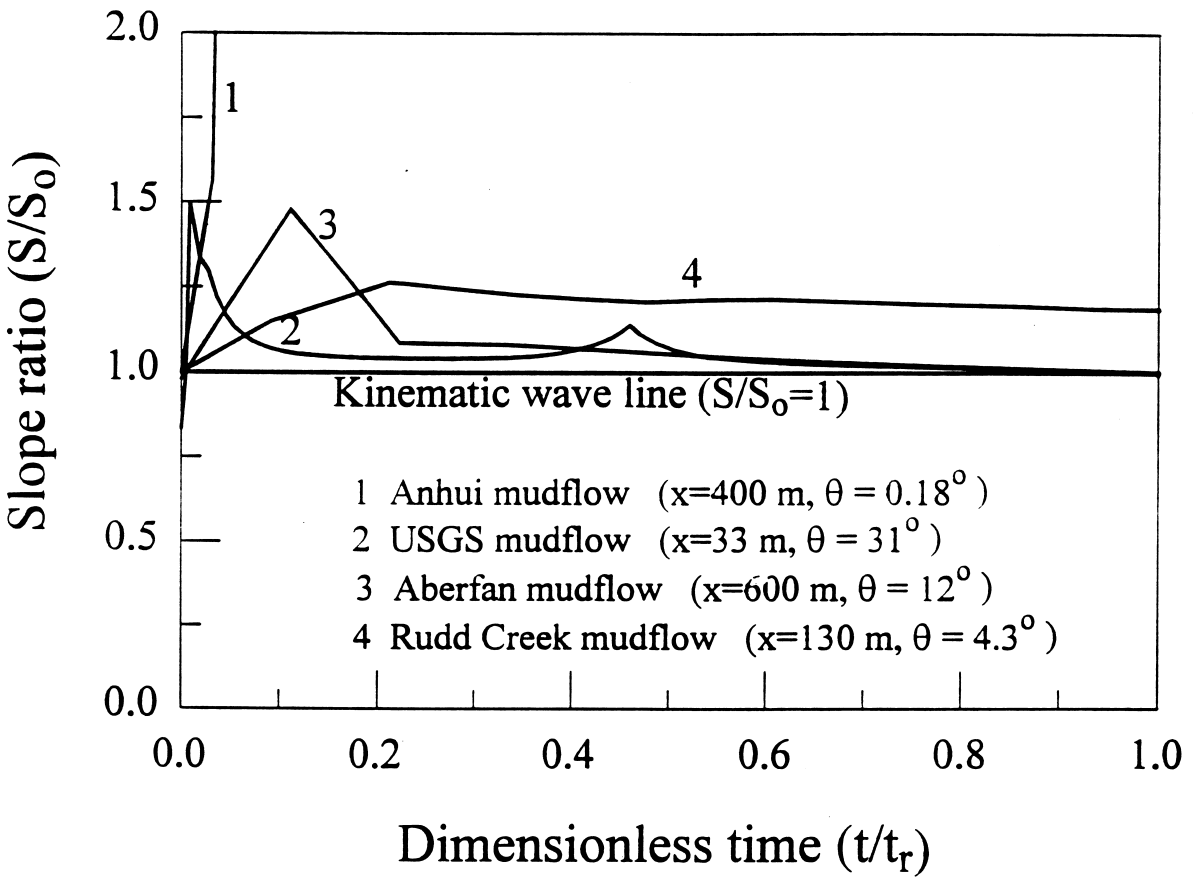

Figure 10 Slope ratio (S/S_o) for 4 cases